energies

MDPI

Article

Frequency Support from a Variable-Speed Wind Turbine Generator Using Different Variable Droop Characteristics

Dejian Yang [1,*], Jingjiao Li [2], Xinsong Zhang [1] and Liang Hua [1,*]

[1] School of Electrical Engineering, Nantong University, Nantong 226019, China; zhang.xs@ntu.edu.cn
[2] Nanjing Institute of Technology, School of Electric Power Engineering, Nanjing 211167, China; jjli@njit.edu.cn
* Correspondence: dejian@ntu.edu.cn (D.Y.); hualiang@ntu.edu.cn (L.H.);
Tel.: +86-1834-502-9980 (D.Y.); Fax: +86-0255-809-9095 (D.Y.)

Received: 31 July 2020; Accepted: 25 August 2020; Published: 31 August 2020

Abstract: Doubly-fed induction generators (DFIGs) are capable of boosting frequency response capability while preventing the rotor speed from stalling during under-frequency disturbances, by employing variable droop characteristics. However, the frequency response capability during over-frequency disturbances is shortened because the potential for storing the kinetic energy is inversely proportional to the variable droop characteristics used for under-frequency disturbances. This paper designs a frequency control method of a DFIG to boost the frequency response capability during over-frequency disturbances while preserving the frequency response capability during under-frequency disturbances, by employing different variable droop characteristics. The effectiveness of the proposed frequency control method is investigated in a test system. The investigation results under five scenarios with different load variations, wind power penetrations and wind conditions clearly demonstrate that the proposed frequency control method suppresses the maximum system frequency deviations. As such, the proposed frequency control method can provide an effective solution for the frequency control ancillary service of a power system with large integrations of wind energy.

Keywords: wind power; system frequency response; over-frequency disturbances; DFIG

1. Introduction

Recently, wind power generation has grown quickly, but it raises issues concerning the stability of an electric power grid. The grid frequency stability is one of challenges caused by a large amount of wind energy integration [1]. This is because power electronic converters interfaced with doubly-fed induction generator (DFIG) decouple the rotor speed from the grid frequency. Accordingly, DFIGs are unable to contribute to the grid frequency support during a disturbance, e.g., a load connection or disconnection [2]. As the wind power penetration increases, the maximum frequency deviation becomes larger [3]. As a result, from the point of view of a power system, conventional synchronous fleets are needed to operate at part-load levels more frequently, or shut down during over-frequency disturbances, which enacts a decreased life cycle and an increased cost [4]; moreover, for an under-frequency disturbance, low-frequency load-shedding relaying is triggered more frequently to prevent further frequency reductions [5]. On the other hand, from the point of view of DFIGs, Chinese and Energinet Grid codes defined the normal frequency production range as from 49.5 s to 50.2 Hz [6,7]. When the grid frequency is more than 50.2 Hz, to protect DFIGs, they should decrease the output power according to the order, or it should be disconnected from the grid in an

emergency situation [6,7]. Therefore, the defense plans of a power system should pay more attention to over-frequency disturbances compared to under-frequency disturbances.

To boost the grid frequency stability, DFIGs are required to supply a frequency control function [8–17]. Many research works focus on designing the frequency control function by utilizing two kinds of energy sources from the DFIG. The first energy source is the reserved power of the DFIG, which is achieved by employing pitch-angle control [10] or over-speed control [11]. This kind of control method requires the DFIG to deviate from the maximum power point tracking (MPPT) operation. Accordingly, significant mechanical energy captured losses are inevitable. Frequent activations of the pitch-angle control might increase the fatigue and mechanical stress of the DFIG; moreover, the response for frequency control is slow because of the mechanical regulation of the pitch-angle control [12]. Another energy source is the rotational kinetic energy produced by a DFIG in supporting the grid frequency by releasing part of the kinetic energy from the rotating blades [12–18]. This strategy is achieved by modifying the rotor side converter (RSC) controller of the DFIG, which means adding the rate of change of frequency (RoCoF) control loop and droop (frequency deviation) control loop [13–15]. The authors of [12] show that the RoCoF loop can emulate the conventional synchronous inertia response to boost the grid frequency's stability; however, this may result in instability because of the noise in the measured grid frequency. As studied in [16], droop control—which emulates the primary frequency response of synchronous generators—can be considered as an alternative inertial response of DFIGs. In [4], the performance of droop control with different constant control gains has been analyzed. A large value of the constant control gain can provide a better performance of frequency response, but it causes the stalling of the rotor speed due to the excessive released energy during under-frequency disturbances. Conversely, a small value can prevent the rotor speed from stalling, but it shortens the contribution of the frequency response. In [17], a stable variable droop gain based on the releasable kinetic energy of DFIGs is suggested. This method can boost the grid frequency response capability while preventing the DFIG from stalling during under-frequency disturbances. However, such droop gain is not suitable for over-frequency disturbances due to the shortened grid frequency response capability. This is because the droop control gain for the rotor at a low speed is less than that for a high-speed rotor, despite the fact that the energy-absorbing potential of a low speed rotor is greater than that of a high speed rotor.

This paper designs a frequency control method for a DFIG that boosts the frequency response capability during over-frequency disturbances, while preserving the frequency response capability for under-frequency disturbances. To this end, the proposed method suggests different variable droop characteristics for over- and under-frequency disturbances, which varies with respect to the rotor speed of the DFIG. This study assumes that DFIGs are operating in MPPT mode prior to disturbance, and are utilizing the rotating turbines of DFIGs for frequency response. The performance of the proposed frequency control method is validated under five scenarios with different load variations, wind power penetrations and wind conditions based on an electromagnetic transient program restructured version (EMTP-RV) simulator.

2. Frequency Response of a Power System

In an electric power system, the grid frequency—which should always be kept within an allowable range—is coupled to the rotational speed of synchronous generators. Accordingly, the grid frequency is reflected as the relationship between the active power generation and the load consumption. The power system is considered as an equivalent synchronous generator, injecting power to loads because synchronous generators are synchronized in power systems [18].

The grid frequency dynamics are governed by the rotor motion equation, as described in (1).

$$J_{sys} \times f_{sys} \times \frac{df_{sys}}{dt} = P_{m\_sys} - P_{e\_sys} \quad (1)$$

where J_{sys} and f_{sys} are the equivalent moment of inertia and grid frequency, respectively. P_{e_sys} and P_{m_sys} are the electrical power and mechanical power of the equivalent synchronous generator.

If a power imbalance occurs in a power system, to counterbalance the power imbalance, the grid frequency decreases as the synchronous generators inherently release the kinetic energy to the grid, or the grid frequency increases as the synchronous generators store the kinetic energy in their rotating masses. Then, synchronous generators increase or decrease their mechanical input power in order to arrest the grid frequency variation on the basis of the measured rotating speed deviation, and stabilize the grid frequency to a quasi-steady state. After that, the grid frequency is recovered to the nominal value by initiating or stopping fast-start units (diesel and open-cycle gas units) [19].

3. Control of a Doubly-Fed Induction Generator

The captured mechanical power from the wind—which is mainly dependent on the blade profile, wind speed, etc.—can be defined as (2) by the actuator disk theory [20].

$$P_m = 0.5\rho A v_w^3 c_P(\lambda, \beta) \tag{2}$$

where ρ represents the air density, A represents the swept area by the turbine, v_w represents the wind speed, λ represents the tip–speed ratio, β represents the pitch angle and c_p represents the power coefficient.

As in [21], the power coefficient is mainly dependent on λ and β, as given by:

$$c_P(\lambda, \beta) = 0.645\{0.00912\lambda + \frac{-5 - 0.4(2.5 + \beta) + 116\lambda_i}{e^{21\lambda_i}}\} \tag{3}$$

$$\lambda_i = \frac{1}{\lambda + 0.08(2.5 + \beta)} - \frac{0.035}{1 + (2.5 + \beta)^3} \tag{4}$$

where λ is given as:

$$\lambda = \frac{\omega_r R}{v_w} \tag{5}$$

c_p retains a maximum value at the optimal λ (λ_{opt}) when $\beta = 0°$. At λ_{opt}, a DFIG can extract the maximum power from wind. Substituting (5) in (2), the active power order for MPPT operation, P_{MPPT}, is represented as:

$$P_{MPPT} = \frac{1}{2}\rho A(\frac{\omega_r R}{\lambda_{opt}})^3 c_{P,\max} = k_g \omega_r^3 \tag{6}$$

where k_g represents a constant coefficient of MPPT operation.

Figure 1 shows the DFIG control system, which includes a pitch angle, RSC, and grid side converter (GSC) controllers. The pitch angle controller deals with the de-loading operation according to the power order, or prevents the rotor speed from exceeding the maximum value. The RSC controller is respectively used to keep the stator voltage and control active power of the electric power grid. The GSC controller adjusts the DC-link voltage at a reference value [22]. Further, a two-mass model is used in this study.

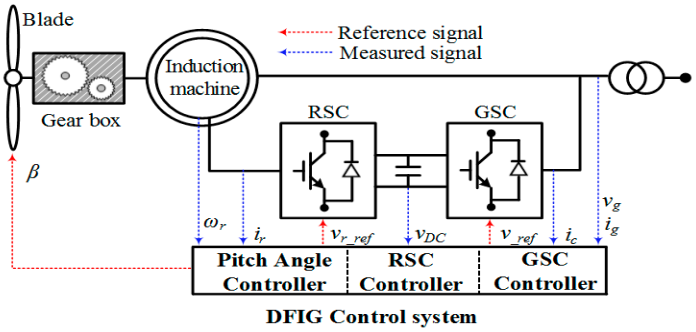

Figure 1. Doubly-Fed Induction Generator configuration.

Figure 2 indicates the power characteristics of the DFIG used in this study. The black dashed lines of Figure 2 reflect the ω_r operating range of a DFIG, which is from 0.70 p.u. (corresponds to $\omega_{\min}$) to 1.25 p.u. (corresponds to $\omega_{\max}$). The red solid line and blue line indicate the MPPT curve and mechanical input power curves with different wind speeds, respectively.

The rotating kinetic energy stored in a DFIG (E_{DFIG}) can be represented as:

$$E_{DFIG} = \frac{1}{2} J_{DFIG} \omega_r^2 \tag{7}$$

where J_{DFIG} means the moment of inertia of a DFIG.

The releasable kinetic energy and storable kinetic energy of a DFIG can be expressed as in (8) and (9):

$$E_{\mathrm{REL}} = \frac{1}{2} J_{DFIG} (\omega_r^2 - \omega_{\min}^2) \tag{8}$$

$$E_{\mathrm{STO}} = \frac{1}{2} J_{DFIG} (\omega_{\max}^2 - \omega_r^2) \tag{9}$$

where E_{REL} and E_{STO} mean the releasable kinetic energy and the storable kinetic energy of a DFIG, respectively.

As shown in Figure 2, E_{REL} is proportional to the rotor speed, whereas E_{STO} is inversely proportional to the rotor speed.

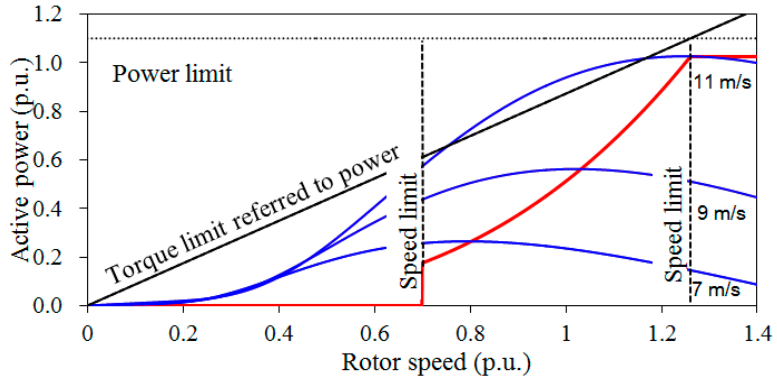

Figure 2. Power characteristics of the doubly-fed induction generator (DFIG) used in this study.

4. Concepts of Frequency Response of a DFIG

To boost the grid frequency response capability during over-frequency disturbances, the output power of the DFIG should be reduced by its storing kinetic energy in itself. Note that the energy-storing capability is an inversely proportional function of the rotor speed; frequent activations of the pitch-angle control should be prevented, thereby reducing the mechanical stress and fatigue of DFIGs.

4.1. Concepts of Conventional Frequency Response Method

Figure 3 displays the diagram of the frequency control method based on the measured frequency deviation. The active power reference (P_{ref}) during the frequency control, which consists of the output power of the MPPT operation (P_{MPPT}) and the output power of the frequency deviation control loop (ΔP_{add}), can be represented as in (10). ΔP_{add} is derived by multiplying the frequency deviation (Δf) by the control gain (K). Therefore, the performance of the frequency response capability of the DFIGs is critically dependent on the control gain, K.

$$\begin{aligned} P_{ref} &= P_{MPPT} + \Delta P_{add} \\ &= P_{MPPT} + \Delta f \times K \end{aligned} \tag{10}$$

As mentioned previously, a constant control gain is suggested in [14]; however, this method cannot compromise the better performance of boosting the grid frequency response and preventing the rotor speed stall. To solve this issue, the authors of [17] suggested a stable variable droop characteristic, which varies with respect to ω_r, as given by:

$$K = AG(\omega_r) = C(\omega_r^2 - \omega_{\min}^2) \tag{11}$$

where C is a constant and decides the performance of the frequency response of the DFIG. $\omega_{\min}$ means the minimum rotor speed of the DFIG.

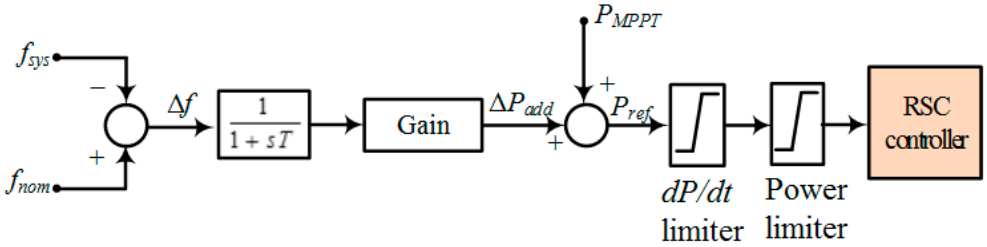

Figure 3. Diagram of the frequency control method.

As in (11), the stable variable droop characteristics are a quadratic function of ω_r. This means that the grid frequency response capability becomes better with the increasing ω_r, because a high speed of the rotor has a better energy-releasing capability than a low speed. In addition, the control gain is set to zero when $\omega_r = \omega_{\min}$, and thus this method can effectively prevent the DFIGs with low rotor speeds from stalling. The use of $AG(\omega_r)$ effectively boosts the frequency response capability during under-frequency disturbances. Nevertheless, the contribution to boosting the energy-storing capability is shortened during over-frequency disturbances. This is because the potential for storing kinetic energy is inversely proportional with respect to ω_r, whereas the control gain used for under-frequency disturbance in (11) is proportion to ω_r.

To produce realistic results, the maximum output limiter and rate limiter are considered [23,24]. The upper limit is the minimum value of the torque and power limitations. The rate limiter is 0.45 p.u./s.

4.2. Concepts of Proposed Frequency Response Method

This paper focuses on boosting the grid frequency response capability by efficiently utilizing the rotating wind turbines, particularly during over-frequency disturbances. To this end, the proposed method employs different variable control characteristics for under- and over-frequency disturbances, which are represented as $AG_{UF}(\omega_r)$ and $AG_{OF}(\omega_r)$, respectively.

Note that $AG_{UF}(\omega_r)$ is set to the same gain as $AG(\omega_r)$ in the conventional frequency control method of [17] so as to maintain the energy-releasing capability during under-frequency disturbances, as shown by the red dashed line in Figure 4. The definition of $AG_{OF}(\omega_r)$ will be explained in the following.

Definition of $AG_{OF}(\omega_r)$

As indicated in Figure 2, the potential for storing energy in a low-speed region of the rotor is greater than that in a high-speed region. Thus, to sufficiently use the rotational kinetic energy, $AG_{OF}(\omega_r)$ should be defined as an inverse proportional function of ω_r, and proportional to the energy-storing capability of a DFIG, which is a symmetric function of $AG_{UF}(\omega_r)$, whereby y = C ($\omega^2_{\max} - \omega^2_{\min}$), as in (11) (see the red solid line in Figure 4).

$$AG_{OF}(\omega_r) = -C(\omega_r^2 - \omega_{\min}^2) + 2C(\omega_{\max}^2 - \omega_{\min}^2) \quad (12)$$

The constant C in (12) is the same as in (11), which is used to adjust the performance of the frequency response of a DFIG. $\omega_{\max}$ means the maximum rotor speed of the DFIG.

The control gain in (12) reflects the fact that $AG_{OF}(\omega_r)$ is greater than $AG_{UF}(\omega_r)$, so that the grid frequency response capability can be boosted compared to the method in [17] during over-frequency disturbances. Furthermore, a large $AG_{OF}(\omega_r)$ is conducive to storing a large amount of kinetic energy in DFIGs; as a result, the ω_r of the DFIGs increases. When an under-frequency disturbance occurs, $AG_{UF}(\omega_r)$ becomes large due to the increased ω_r, and thus a large amount of energy can be injected into the grid for reducing the maximum frequency deviation. Such performance can be observed in the Simulation Results Section (Case 3).

C in (11) and (12) can be determined as having different values depending on the design purposes. This paper aims to determine the droop characteristics of the DFIG depending on the kinetic energy stored in the rotating masses, so that the DFIG releases a large amount of kinetic energy to suppress the maximum frequency deviation during the over-frequency disturbance. However, if the DFIG releases too much kinetic energy while performing frequency control because of a large gain, the rotor speed might reach the minimum operating rotor speed (ω min). In this case, the DFIG has to disable the inertial control to protect itself. This might cause a significant power reduction in the DFIG, and further causes a subsequent frequency drop in the power grid. Therefore, this paper determines the droop control characteristics so that they prevent the rotor speeds of the DFIGs from reaching $\omega_{\min}$ during an under-frequency disturbance. For the over-frequency disturbance, if the DFIG absorbs too much kinetic energy while performing frequency control, the pitch-angle might be started up frequently, which might increase the mechanical stress and fatigue of the DFIG. Thus, this paper determines the droop control characteristics so that they avoid the frequent activations of the pitch-angle control during under-frequency disturbances.

Note that the important part of the proposed frequency control method is how to determine the end-points and shaping function of $AG_{OF}(\omega_r)$. For convenience, (0.7, 2C ($\omega^2_{\max} - \omega^2_{\min}$)) corresponding to Point A in Figure 4 and (1.25, C ($\omega^2_{\max} - \omega^2_{\min}$)) corresponding to Point B in Figure 4 are selected as the end-points for $AG_{OF}(\omega_r)$; furthermore, a symmetric function of $AG_{UF}(\omega_r)$ around y = C ($\omega^2_{\max} - \omega^2_{\min}$) is selected for the shaping function of $AG_{OF}(\omega_r)$. As a result, $AG_{OF}(\omega_r)$ is more able than $AG_{UF}(\omega_r)$ to boost the frequency support capability.

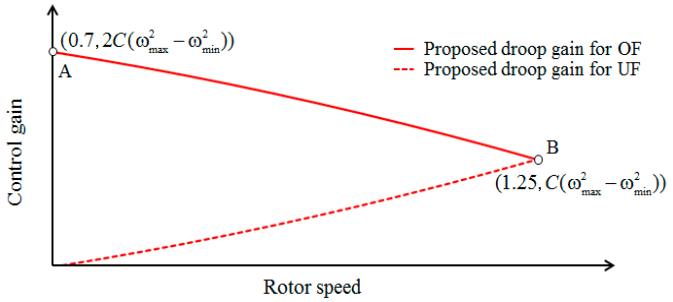

Figure 4. Droop characteristics of the proposed frequency control method.

5. Simulation Studies

To verify the performance of the proposed frequency control method, a test model system consisting of five conventional synchronous generators, a static load, a motor load and an aggregated DFIG-based wind farm is used, as shown in Figure 5. All synchronous generators are implemented with IEEEG1 and IEEEX1models for frequency and voltage regulation. The droop settings for all synchronous generators are set to 5%.

In Case 1, Case 2 and Case 5, a static load (40 MW) is suddenly connected to the test system at 60.0 s and disconnected at 100.0 s; in Case 3, a static load (40 MW) is suddenly disconnected from the test system at 60.0 s and connected at 100.0 s. In Case 4, a static load (40 MW) is suddenly connected to the test system at 60.0 s and 100.0 s. Detailed simulation results for these scenarios are discussed in the following five subsections. Moreover, it is assumed that the DFIG is subject to a command wind condition (10 m/s and 8.0 m/s), and keeps fixed during simulation.

The performance of the proposed method is compared then to the method with stable droop characteristics (which is denoted as the conventional method) [17] and MPPT operation (which means no frequency response from the DFIG). In the proposed method and conventional method, the value of C in (11) and (12) is set to 50. It is noteworthy that the value of C provides only an example here, and can be set to different values.

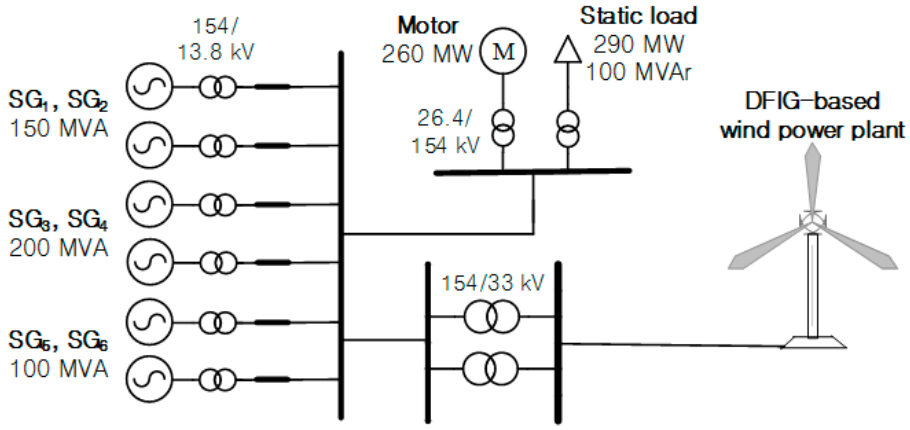

Figure 5. Model system with a DFIG-based wind power plant.

5.1. Case 1: 40 MW Load Connection at 60.0 s and 40 MW Load Disconnection at 100.0 s, Wind Speed Is 10.0 m/s, Wind Power Penetration Is 16.7%

As shown in Figure 6a, the maximum frequency deviations for the under-frequency disturbance of the proposed method, the conventional method and the MPPT operation are 0.245 Hz, 0.245 Hz and 0.358 Hz, respectively. The maximum frequency deviation during the under-frequency disturbance in the proposed method is the same as in the conventional method, due to the employment of the same control gain, whereas this is less in the MPPT operation by 0.157 Hz. The reason is that more kinetic energy is released from the DFIG, so that the active power injection is greater than in the MPPT operation by around 63.0 s, as displayed in Figure 6a,b.

The maximum frequency deviations for the over-frequency disturbance in the proposed method, conventional method and MPPT operation are 0.138 Hz, 0.168 Hz and 0.254 Hz, respectively. The maximum frequency deviation during the over-frequency disturbance of the proposed method is 0.030 Hz and 0.116 Hz less than that of the conventional method and the MPPT operation, respectively. This is because more kinetic energy is stored in the DFIG at around 103.0 s due to the large control gain, as displayed in Figure 6a–d.

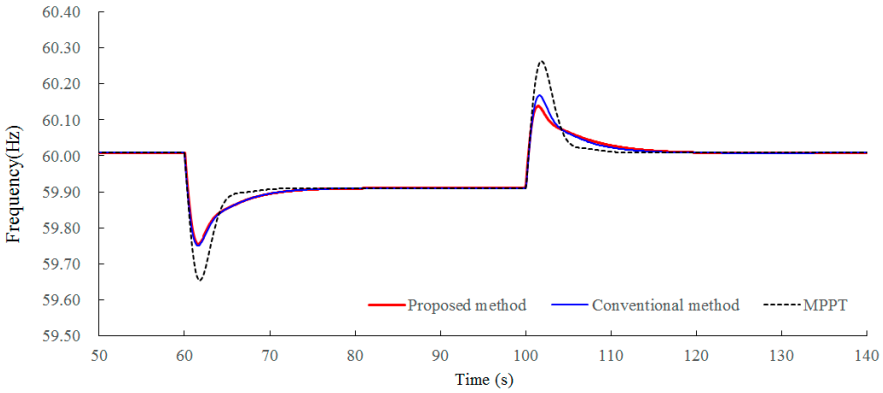

(**a**)

Figure 6. *Cont.*

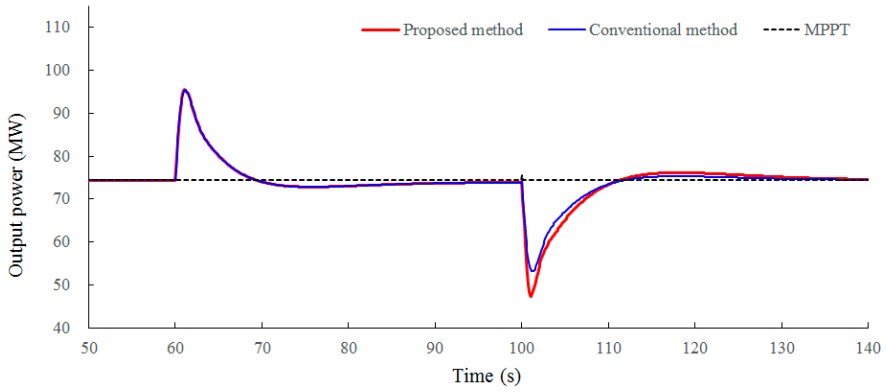

(**b**)

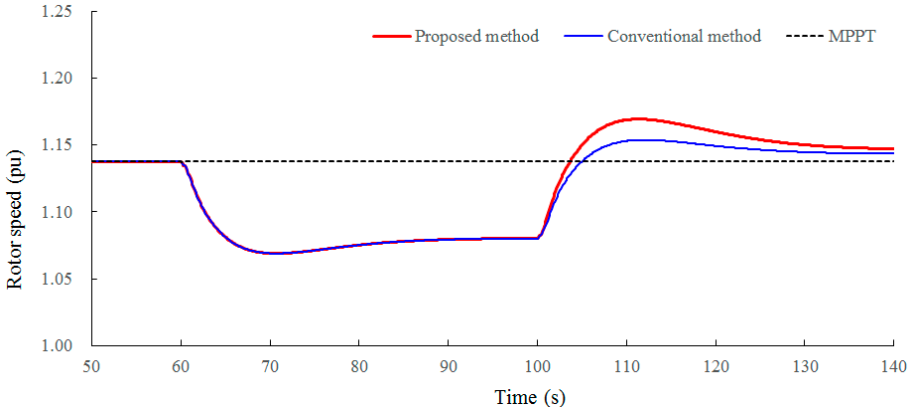

(**c**)

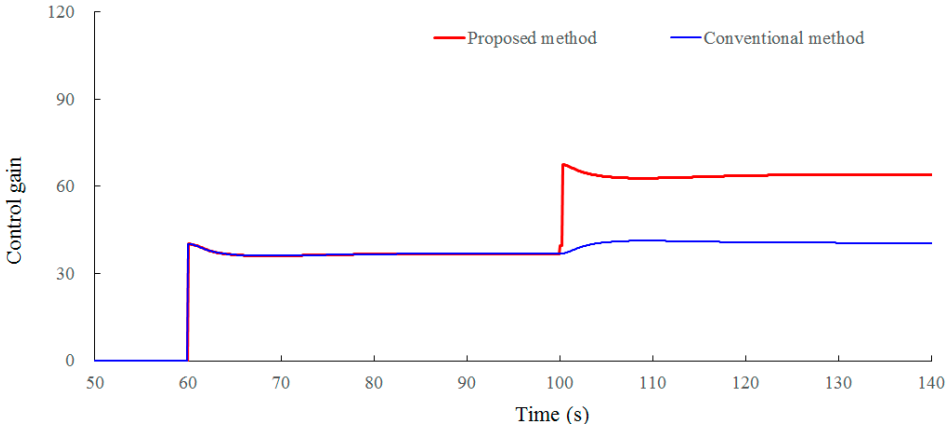

(**d**)

Figure 6. *Cont.*

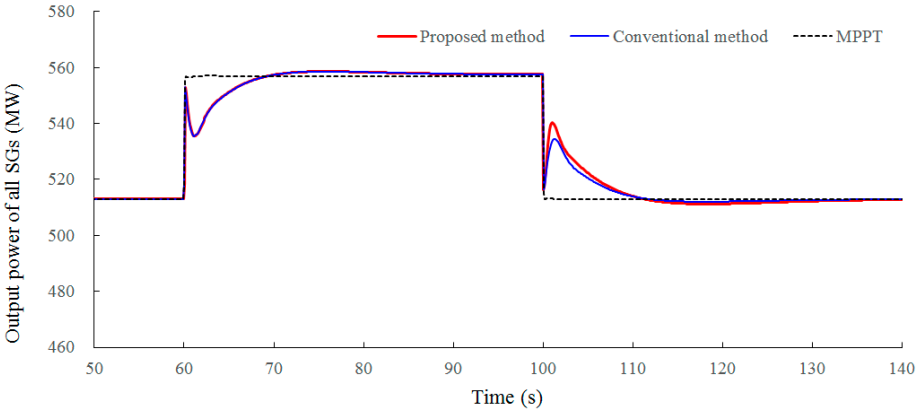

(**e**)

Figure 6. Simulations for Case 1: (**a**) System frequencies; (**b**) Active powers; (**c**) Rotor speeds; (**d**) Control gain; (**e**) Output power of all synchronous generators.

As shown in Figure 6e, the output power of the synchronous generators in the MPPT operation increases to 513 MW at 60.0 s, because no contribution is provided by the DFIGs and the power deficit is supplied by all synchronous generators. Accordingly, the grid frequency decreases to release the kinetic energy from the synchronous generators, so as to compensate for the power deficit. The output power of the synchronous generators is reduced by storing the kinetic energy in the synchronous generators at 100.0 s. As a result, the grid frequency increases. In the conventional method, due to the contribution from the DFIG, the output power increase and decrease of the synchronous generators are less than those of the MPPT operation. In the proposed method, the output increase of the synchronous generators is the same as in the conventional method, due to there being the same control gain, and the decrease in the synchronous generators is less than that in the conventional method because the proposed method provides more contributions from the DFIG for the frequency response during the over-frequency disturbance. Accordingly, the variation in the grid frequency during the over-frequency disturbances in the proposed method is less than that in the conventional method, as shown in Figure 6a.

5.2. Case 2: 40 MW Load Connection at 60.0 s and 40 MW Load Disconnection at 100.0 s, Wind Speed Is 8.0 M/S, Wind Power Penetration Is 16.7%

Figure 7 shows the results for Case 2, which is identical to Case 1 except for the wind conditions. As shown in Figure 7a, the maximum frequency deviations for the under-frequency disturbance of the proposed method, the conventional method and the MPPT operation are 0.308 Hz, 0.308 Hz and 0.358 Hz, respectively. The maximum frequency deviation during the under-frequency disturbance in the proposed method is the same as that in the conventional method, whereas it is less than that in the MPPT operation by 0.050 Hz. This is because more kinetic energy is released from the DFIG, so that the active power injection is greater than in the MPPT operation at around 63.0 s, as displayed in Figure 7a,b and as in Case 1. The maximum frequency deviation of the MPPT operation is the same as in Case 1 due to the fact that all the active power is injected from the synchronous generators. The frequency deviations of the conventional method and proposed method are greater than those in Case 1, because less power is injected into the grid due to the smaller controller gain.

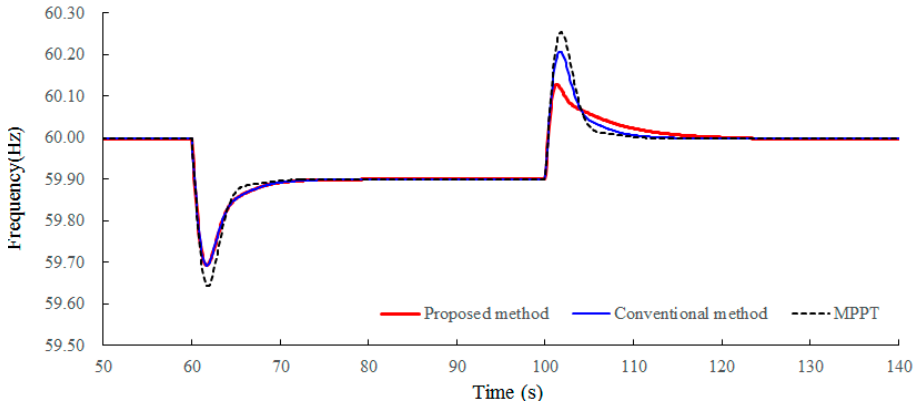

(**a**)

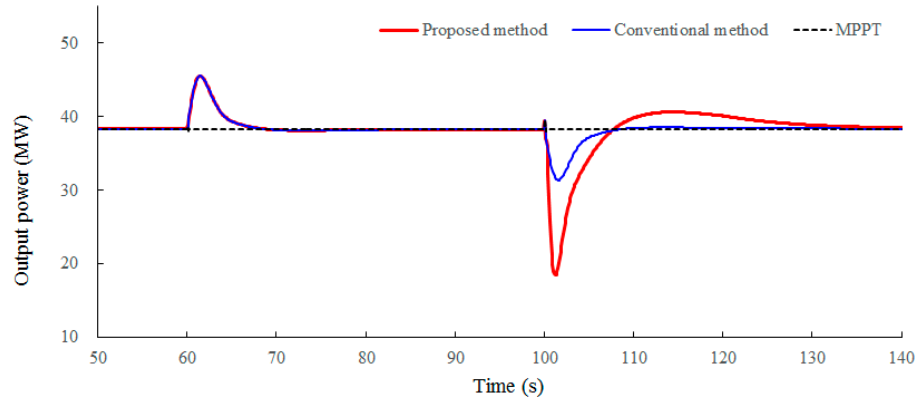

(**b**)

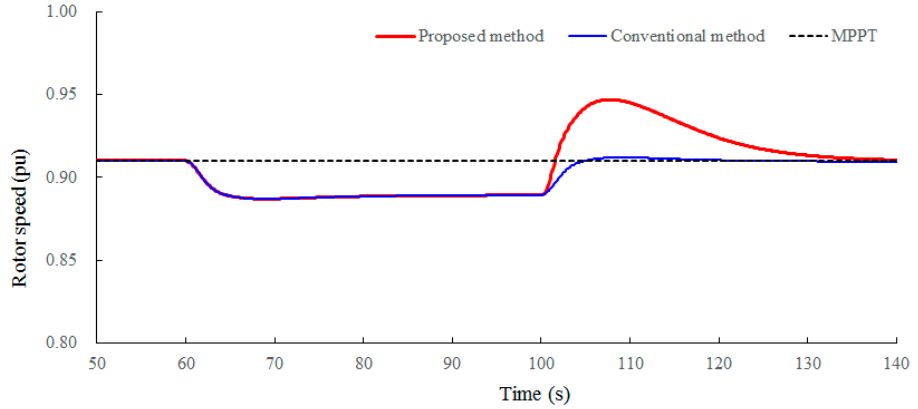

(**c**)

Figure 7. *Cont.*

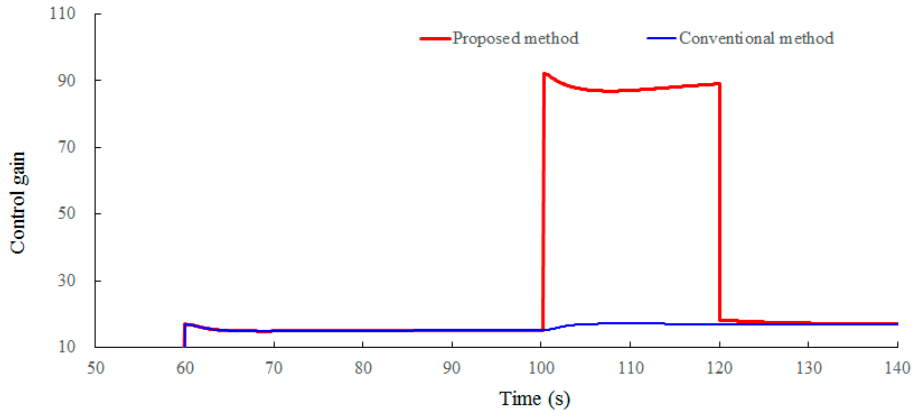

(**d**)

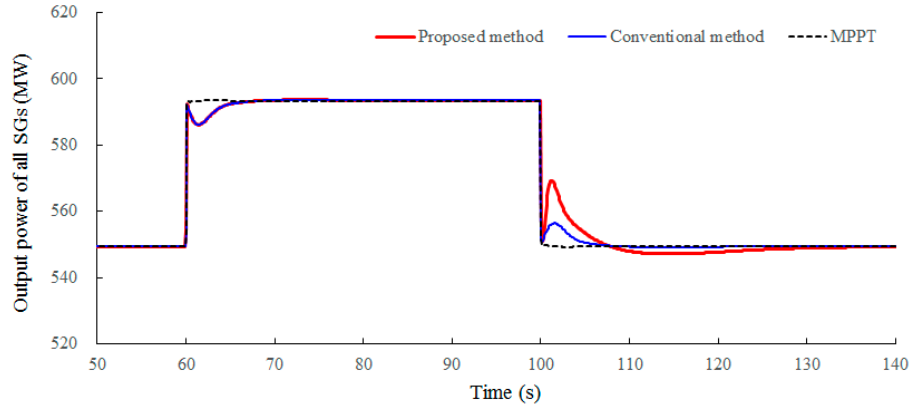

(**e**)

Figure 7. Results for Case 2: (**a**) System frequencies; (**b**) Active powers; (**c**) Rotor speeds; (**d**) Control gain; (**e**) Output power of all synchronous generators.

The maximum frequency deviations for the over-frequency disturbance in the proposed method, conventional method and MPPT operation are 0.185 Hz, 0.207 Hz and 0.254 Hz, respectively. The maximum frequency deviation during the over-frequency disturbance of the proposed method is 0.022 Hz and 0.169 Hz less than that of the conventional method and the MPPT operation, respectively. This is because more kinetic energy is stored in the DFIG at around 103.0 s due to the large control gain. The frequency deviations of the conventional method and proposed method are greater than those in Case 1 because less power is absorbed.

As shown in Figure 7e, the output power of the synchronous generators of the MPPT operation increase to 550 MW at 60.0 s because no contribution is provided from the DFIGs, and the power deficit is supplied by all synchronous generators. Accordingly, the grid frequency decreases to release the kinetic energy from the synchronous generators, and the output power of the synchronous generators is decreased by storing the kinetic energy in the synchronous generators at 100.0 s. In the conventional method, due to the contribution from the DFIG, the output power increase and decrease of the synchronous generators are less than those of the MPPT operation. In the proposed method, the output increase of the synchronous generators is the same as in the conventional method, due to there being the same control gain; the decrease in the synchronous generators is less than that in the conventional method because the proposed method provides more contributions from the DFIG for frequency response during the over-frequency disturbance. Accordingly, the variation in the grid frequency during the over-frequency disturbances in the proposed method is suppressed more so than that in the conventional method, as shown in Figure 7a.

5.3. Case 3: 40 MW Load Disconnection at 60.0 s and 40 MW Load Connection at 100.0 s, Wind Speed Is 8.0 M/S, Wind Power Penetration Is 16.7%

Figure 8 shows the results for Case 3, which is identical to Case 1 except for the load variations. As shown in Figure 8a, the maximum frequency deviations for the over-frequency disturbance in the proposed method, conventional method and MPPT operation are 0.191 Hz, 0.300 Hz and 0.352 Hz, respectively. As in Case 2, the proposed method can suppress the maximum frequency deviations. This is because more kinetic energy is stored in the DFIGs during the over-frequency disturbance.

The maximum frequency deviation for the under-frequency disturbance in the proposed method is 0.143 Hz, which is less than those of the conventional method and the MPPT operation by 0.062 Hz and 0.118 Hz, respectively (see Figure 8a). This is because the control gain of the proposed method is greater than that in the conventional method due to the higher rotor speed, as shown in Figure 8c,d. Unlike in the conventional method, even if the same droop control characteristic is used, the proposed method can reduce the maximum frequency deviation.

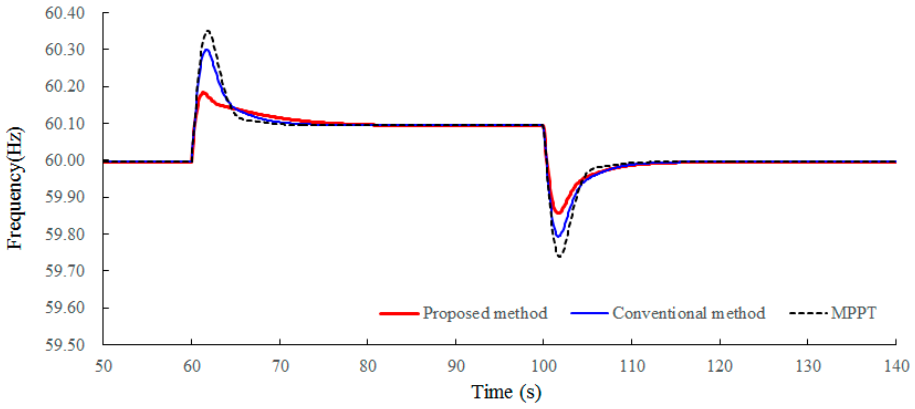

(**a**)

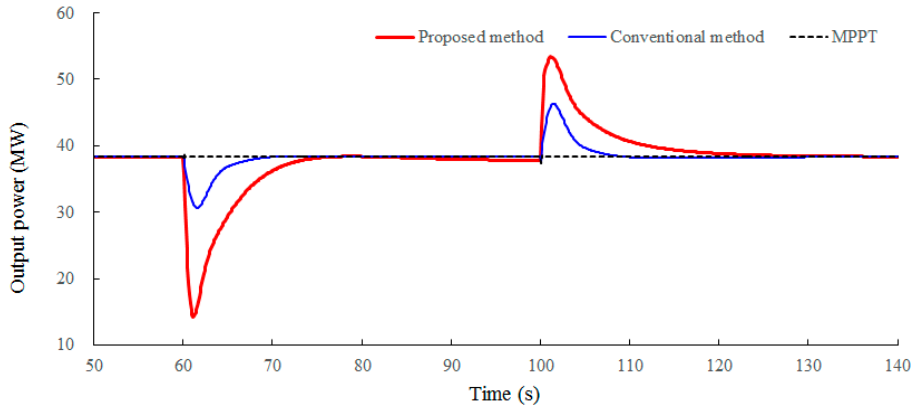

(**b**)

Figure 8. *Cont.*

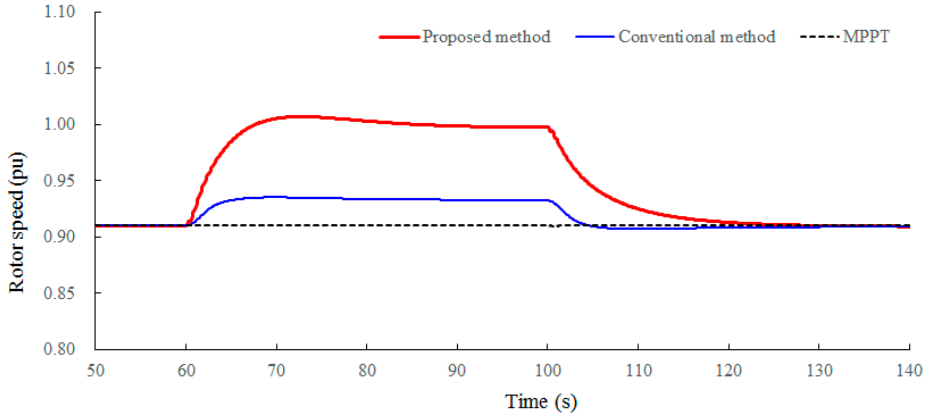

(**c**)

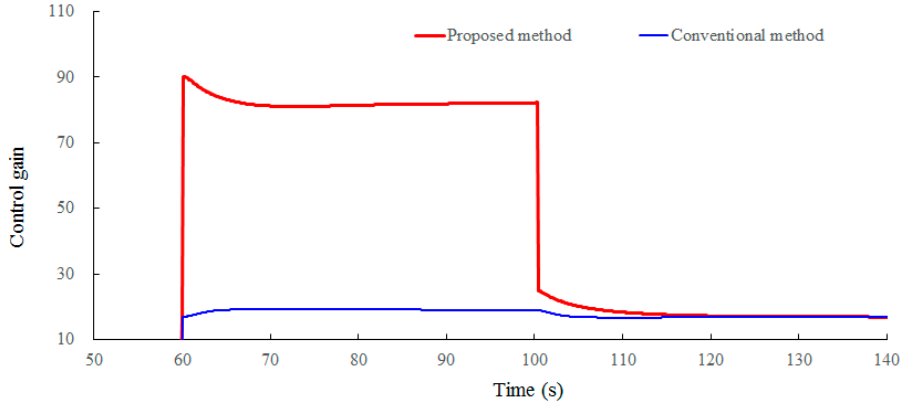

(**d**)

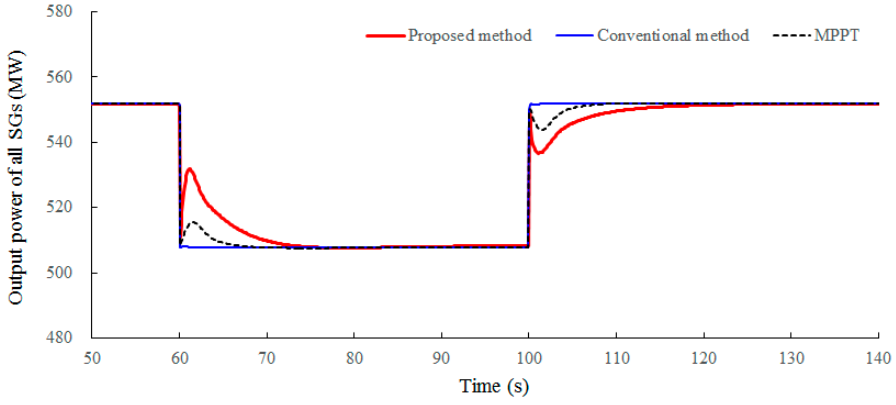

(**e**)

Figure 8. Results for Case 3: (**a**) System frequencies; (**b**) Active powers; (**c**) Rotor speeds; (**d**) Control gain; (**e**) Output power of all synchronous generators.

As shown in Figure 8e, the output power of the synchronous generators in the MPPT operation decreases to 510 MW at 60.0 s due to the fact that no contribution is provided from the DFIG, and all additional power is stored in the synchronous generators. Accordingly, the grid frequency increases due to the stored kinetic energy. At 100.0 s, the output powers of the synchronous generators is increased to 550 MW by releasing the kinetic energy from the synchronous generators, such that the grid frequency decreases. As shown in Figure 8e, the amounts of output power decrease and increase in the synchronous generators in the proposed method are less than those in the conventional method, because

the proposed method provides a greater contribution from the DFIG for frequency control. Accordingly, the variation in the grid frequency during the over-frequency and under-frequency disturbances in the proposed method is less than that in the conventional method, as shown in Figure 8a.

5.4. Case 4: 40 MW Load Disconnection at 60.0 s and 40 MW Load Disconnection at 100.0 s, Wind Speed Is 8.0 M/S, Wind Power Penetration Is 16.7%

Figure 9 shows the results for Case 4, which is identical to Case 3 except for load variations. Thus, the simulation results prior to 100 s are the same as those in Case 3. As shown in Figure 9a, the maximum frequency deviations for the second over-frequency disturbance in the proposed method, conventional method and MPPT operation are 0.290 Hz, 0.390 Hz and 0.453 Hz, respectively. The maximum frequency deviation for the second disturbance of the proposed method is greater than that of the conventional method and the MPPT operation by 0.010 Hz and 0.163 Hz, respectively. As in Case 3, the proposed method can effectively suppress the maximum frequency deviations. This is due to the fact that more kinetic energy can be stored in the DFIGs during the over-frequency disturbance by employing the control in (12).

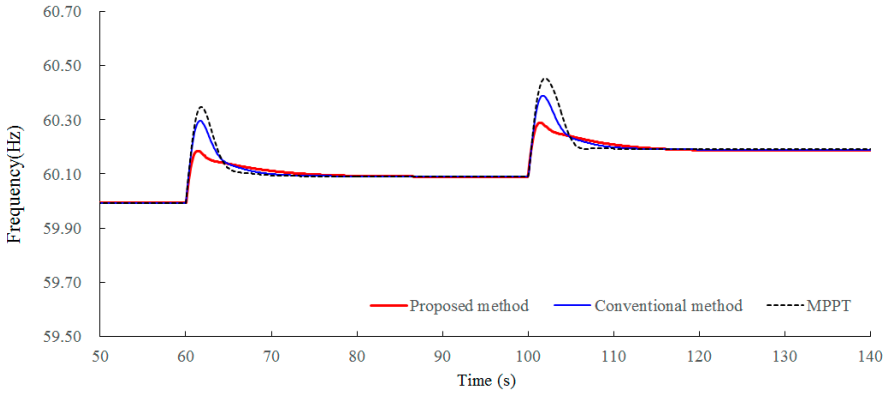

(**a**)

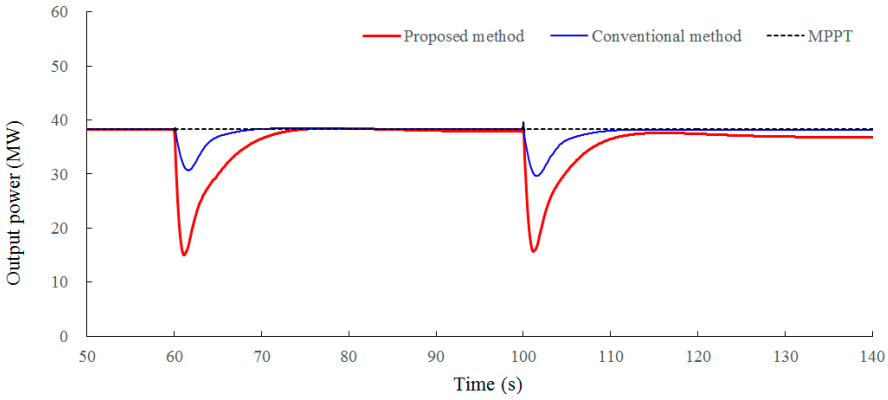

(**b**)

Figure 9. *Cont.*

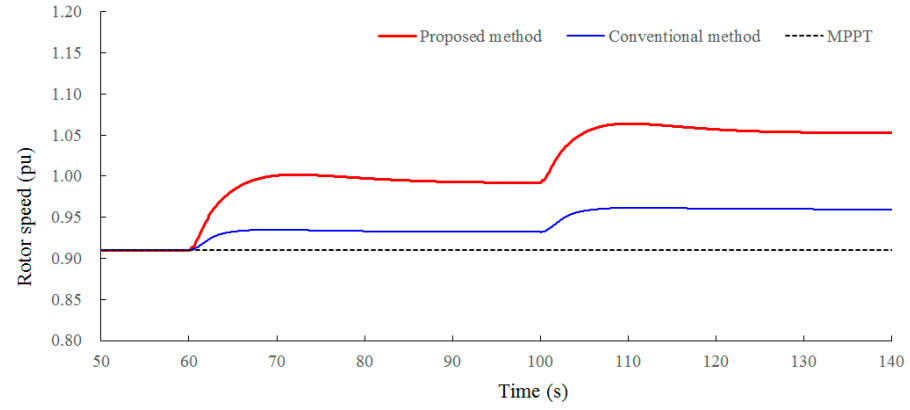

(**c**)

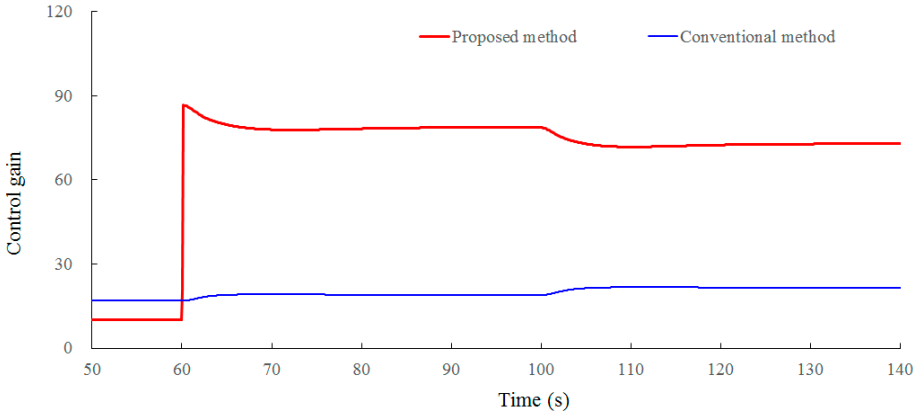

(**d**)

Figure 9. Simulations for Case 4: (**a**) System frequencies; (**b**) Active powers; (**c**) Rotor speeds; (**d**) Control gain.

5.5. Case 5: 40 MW Load Disconnection at 60.0 s and 40 MW Load Connection at 100.0 s, Wind Speed Is 8.0 M/S, Wind Power Penetration Is 25%

Figure 10 shows the results for Case 5, which is identical to Case 2 except for the wind power penetration level. As shown in Figure 10a, the maximum frequency deviation of the under-frequency disturbance in the proposed method is the same as in the conventional method, and is larger than that in the MPPT operation, as in Case 2 with low wind power penetration. The frequency deviation during the over-frequency disturbance is greater than that of the conventional method and MPPT operation.

Compared to the maximum frequency deviations of Case 2, the maximum frequency deviations of the MPPT operation during the over-frequency and under-frequency disturbances become large due to the reduced frequency regulation capability and inertia constant. For the conventional method and proposed method, the maximum frequency deviations are reduced because more active power is injected into the grid or absorbed into the DFIGs. Further, the improvement of the proposed method is greater than that in the conventional method due to the larger control gain in the over-frequency disturbance, as shown in Figures 7 and 10.

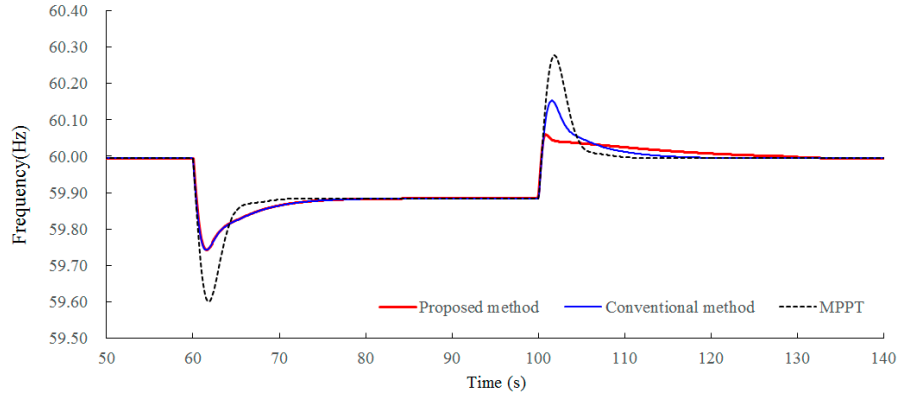

(**a**)

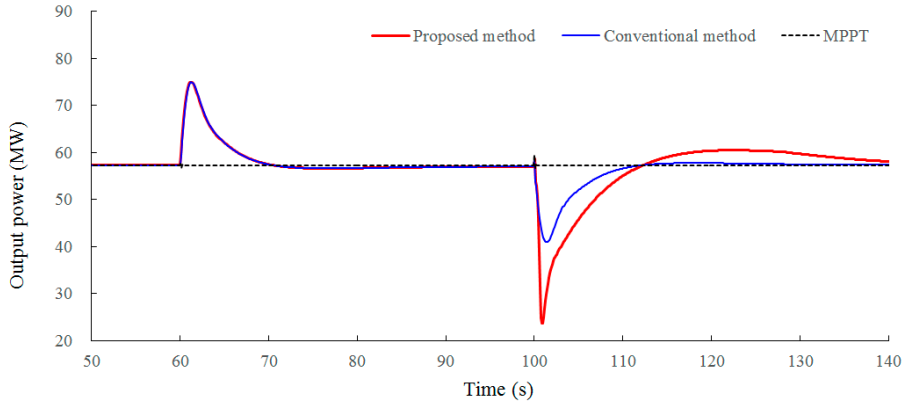

(**b**)

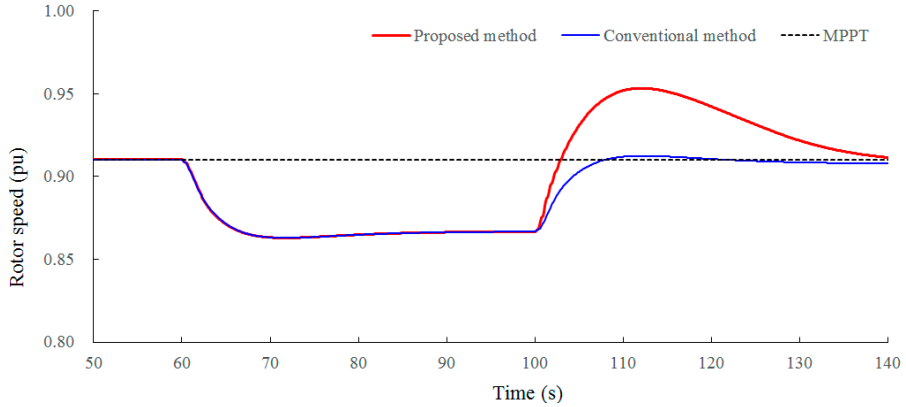

(**c**)

Figure 10. Simulations for Case 5: (**a**) System frequencies; (**b**) Active powers; (**c**) Rotor speeds.

6. Conclusions

This paper designs a frequency control method for the DFIG that can boost the frequency response capability by using different variable droop characteristics. To boost the frequency response capability during the over-frequency disturbance, the variable control characteristics are determined as an inverse-proportional function of the rotor speed. To maintain the frequency response capability of the conventional method during the under-frequency disturbance, the same variable control characteristics are used.

The simulation results for five scenarios with different load variations, wind conditions and wind power penetrations clearly demonstrate that the proposed method effectively suppresses the maximum frequency deviation by using different variable droop characteristics, particularly for over-frequency disturbances. Therefore, the proposed method can provide a solution for the frequency control ancillary service of power systems with large integrations of wind energy.

The novelties are that this paper suggests different droop control characteristics for frequency support during over-frequency and under-frequency disturbance. Further, the control droop characteristic during the over-frequency disturbance is determined based on the potential for storing the kinetic energy in the DFIGs. The advantages of the proposed method are that it suppresses the maximum frequency deviation by using rotor speed-dependent control gains, and it further avoids unnecessary control actions for over-frequency and under-frequency disturbances.

Author Contributions: D.Y. proposed the methodology and simulation tests. D.Y., J.L., X.Z., and L.H. dealt with writing, reviewing and editing. All authors have read and agreed to the published version of the manuscript.

Funding: This work was supported by the Application research program of Nantong City (JC2019092), and National Natural Science Foundation of China (51877112).

Conflicts of Interest: The authors declare no conflict of interest.

References

1. Ackermann, T. Overview of Integration Studies—Methodologies and Results. In *Wind Power in Power System*, 2nd ed.; John Wiley & Sons, Ltd.: West Sussex, UK, 2012.
2. Bevrani, H. Real power compensation and frequency control. In *Robust Power System Frequency Control*; Springer Science Business Media, LLC: New York, NY, USA, 2009; pp. 15–37.
3. Lalor, G.; Mullane, A.; O'Malley, M. Frequency Control and Wind Turbine Technologies. *IEEE Trans. Power Syst.* **2005**, *20*, 1905–1913. [CrossRef]
4. Van De Vyver, J.; De Kooning, J.D.M.; Meersman, B.; Vandevelde, L.; VanDoorn, T.L. Droop Control as an Alternative Inertial Response Strategy for the Synthetic Inertia on Wind Turbines. *IEEE Trans. Power Syst.* **2015**, *31*, 1129–1138. [CrossRef]
5. Delfino, B.; Massucco, S.; Morini, A.; Scalera, P.; Silvestro, F. Implementation and comparison of different under frequency load-shedding schemes. In Proceedings of the IEEE Summer Meeting 2001, Vancouver, BC, Canada, 15–19 July 2001.
6. Standardization Administration of China. *Technical Rule for Connecting to Power System, GB/T19963-2011*; Standardization Administration of China: Beijing, China, 2011.
7. Energinet.dk. *Technical Regulation 3.2.5 for Wind Power Plants with a Power Output Greater Than 11 kW*; Energinet: Fredericia, Denmark, 2010.
8. National Grid. *Grid Code Review Panel Paper, Future Frequency Response Services*; National Grid: London, UK, 2010.
9. Hydro Québec TransÉnergie. *Transmission Provider Technical Requirements for the Connection of Power Plants to the Hydro Québec Transmission System*; Hydro Québec TransÉnergie: Montréal, QC, Canada, 2009.
10. Kamel, R.M.; Chaouachi, A.; Nagasaka, K. Three Control Strategies to Improve the Microgrid Transient Dynamic Response during Isolated Mode: A Comparative Study. *IEEE Trans. Ind. Electron.* **2012**, *60*, 1314–1322. [CrossRef]
11. Vidyanandan, K.V.; Senroy, N. Primary frequency regulation by deloaded wind turbines using variable droop. *IEEE Trans. Power Syst.* **2012**, *28*, 837–846. [CrossRef]
12. Li, Y.; Xu, Z.; Wong, K.P. Advanced Control Strategies of PMSG-Based Wind Turbines for System Inertia Support. *IEEE Trans. Power Syst.* **2016**, *32*, 3027–3037. [CrossRef]
13. Ekanayake, J.; Jenkins, N. Comparison of the Response of Doubly Fed and Fixed-Speed Induction Generator Wind Turbines to Changes in Network Frequency. *IEEE Trans. Energy Convers.* **2004**, *19*, 800–802. [CrossRef]
14. Morren, J.; Pierik, J.; De Haan, S.W. Inertial response of variable speed wind turbines. *Electr. Power Syst. Res.* **2006**, *76*, 980–987. [CrossRef]
15. Morren, J.; De Haan, S.; Kling, W.L.; Ferreira, J. Wind Turbines Emulating Inertia and Supporting Primary Frequency Control. *IEEE Trans. Power Syst.* **2006**, *21*, 433–434. [CrossRef]

16. Zhao, J.; Lyu, X.; Fu, Y.; Hu, X.; Li, F. Coordinated Microgrid Frequency Regulation Based on DFIG Variable Coefficient Using Virtual Inertia and Primary Frequency Control. *IEEE Trans. Energy Convers.* **2016**, *31*, 833–845. [CrossRef]
17. Lee, J.; Jang, G.; Muljadi, E.; Blaabjerg, F.; Chen, Z.; Kang, Y.C. Stable Short-Term Frequency Support Using Adaptive Gains for a DFIG-Based Wind Power Plant. *IEEE Trans. Energy Convers.* **2016**, *31*, 1068–1079. [CrossRef]
18. Kim, J.; Muljadi, E.; Gevorgian, V.; Hoke, A. Dynamic Capabilities of an Energy Storage-Embedded DFIG System. *IEEE Trans. Ind. Appl.* **2019**, *55*, 4124–4134. [CrossRef]
19. Lyu, X.; Xu, Z.; Zhao, J.; Wong, K.P. Advanced frequency support strategy of photovoltaic system considering changing working conditions. *IET Gener. Transm. Distrib.* **2018**, *12*, 363–370. [CrossRef]
20. Sørensen, P.; Hansen, A.D.; Iov, F.; Blaabjerry, F.; Donovan, M.H. *Wind Farm Models and Control Strategies*; Report Risø-R-1464(EN); Risø National Laboratory: Roskilde, Denmark, 2005.
21. Ajjarapu, V.; McCalley, J.D.; Rover, D.; Wang, Z.; Wu, Z. Novel Sensorless Generator Control and Grid Fault Ride-Through Strategies for Variable-Speed Wind Turbines and Implementation on a New Real-Time Simulation Platform. Ph.D. Thesis, Department of Electrical and Computer Engineering, Iowa State University, Ames, IA, USA, 2010.
22. Fernández-Ramírez, L.M.; Garcia, C.; Jurado, F. Comparative study on the performance of control systems for doubly fed induction generator (DFIG) wind turbines operating with power regulation. *Energy* **2008**, *33*, 1438–1452. [CrossRef]
23. Clark, K.; Miller, N.W.; Sanchez-Gasca, J.J. *Modeling of GE Wind Turbine-Generators for Grid Studies*; General Electric Report; Version 4.5; General Electric international Inc.: New York, NY, USA, 2010.
24. Eisa, S.A. Modeling dynamics and control of type-3 DFIG wind turbines: Stability, Q Droop function, control limits and extreme scenarios simulation. *Electr. Power Syst. Res.* **2019**, *166*, 29–42. [CrossRef]